Korean Journal of Radiology

KJR

Clinical Features and Radiological Findings of Adenovirus Pneumonia Associated with Progression to Acute Respiratory Distress Syndrome: A Single Center Study in 19 Adult Patients

Min Jae Cha, MD[1], Myung Jin Chung, MD[2], Kyung Soo Lee, MD[2], Tae Jung Kim, MD[2], Tae Sung Kim, MD[2], Semin Chong, MD[1], Jungho Han, MD[3]

[1]Department of Radiology, Chung-Ang University Hospital, Chung-Ang University College of Medicine, Seoul 06973, Korea; [2]Department of Radiology and Center for Imaging Science, Samsung Medical Center, Sungkyunkwan University School of Medicine, Seoul 06351, Korea; [3]Department of Pathology, Samsung Medical Center, Sungkyunkwan University School of Medicine, Seoul 06351, Korea

Objective: To describe radiologic findings of adenovirus pneumonia and to understand clinico-radiological features associated with progression to acute respiratory distress syndrome (ARDS) in patients with adenovirus pneumonia.
Materials and Methods: This study included 19 patients diagnosed with adenovirus pneumonia at a tertiary referral center, in the period between March 2003 and April 2015. Clinical findings were reviewed, and two radiologists assessed imaging findings by consensus. Chi-square, Fisher's exact, and Student's t tests were used for comparing patients with and without subsequent development of ARDS.
Results: Of 19 patients, nine were immunocompromised, and 10 were immunocompetent. Twelve patients (63%) progressed to ARDS, six of whom (32%) eventually died from the disease. The average time for progression to ARDS from symptom onset was 9.6 days. Initial chest radiographic findings were normal (n = 2), focal opacity (n = 9), or multifocal or diffuse opacity (n = 8). Computed tomography (CT) findings included bilateral (n = 17) or unilateral (n = 2) ground-glass opacity with consolidation (n = 14) or pleural effusion (n = 11). Patients having subsequent ARDS had a higher probability of pleural effusion and a higher total CT extent compared with the non-ARDS group (p = 0.010 and 0.007, respectively). However, there were no significant differences in clinical variables such as patient age and premorbid condition.
Conclusion: Adenovirus pneumonia demonstrates high rates of ARDS and mortality, regardless of patient age and premorbid conditions, in the tertiary care setting. Large disease extent and presence of pleural effusion on CT are factors suggestive of progression to ARDS.
Keywords: *Adenovirus; Pneumonia; Acute respiratory distress syndrome; Chest radiograph; CT*

INTRODUCTION

Adenovirus is a well-known pathogen of mild upper

respiratory tract illness which is usually self-limited. In pediatric patients, adenovirus pneumonia can present with the features of bacterial pneumonia (1). Many cases of fatal adenovirus respiratory infection in immune-suppressed adults have been described in the literature. Because humoral and cellular immunity are generally important in overcoming viral infection, life-threatening adenovirus pneumonia in patients with defective or deficient T-cell immunity, such as those with bone marrow or solid organ transplant, malignant neoplasm, or AIDS, has been reported (2-5). However, there have been a few cases of adenovirus pneumonia in immunocompetent adults. Historically, epidemics and outbreaks of adenovirus pneumonia in military recruits and health care facilities have been

described (6-9). These cases have raised concerns about adenovirus infection in the general population, but there is still limited information on the condition.

We had encountered several patients in our clinical practice with adenovirus pneumonia that rapidly progressed to respiratory failure, and we thought that it was worthwhile to report the clinical and radiological spectra of adenovirus pneumonia in civilian adults. Furthermore, if any clinico-radiological factors appeared to foreshadow the development of acute respiratory distress syndrome (ARDS), aggressive treatment and careful follow-up evaluation can be prepared in advance. Thus, the aim of our study was to identify the incidence, clinical features, survival outcome, and radiological findings of adenovirus pneumonia acquired in the community. We also compared clinico-radiological factors between patients with and without ARDS in order to determine possible predictors for patients who might develop respiratory failure.

MATERIALS AND METHODS

The institutional review board approved our retrospective study, and written informed consent was waived for the use of patients' medical and imaging data. All of the patients' information was anonymized prior to the analysis.

Study Population

We identified 19 adult patients (14 males and 5 females; median age, 38 years) who were diagnosed with adenovirus pneumonia between March 2003 and April 2015 in a single tertiary-referral hospital. All patients underwent Gram stains, bacterial and fungal cultures of blood and urine. Sputum was stained and cultured for bacteria, mycobacteria, and fungi. Specimens from patients who underwent bronchoscopy with the collection of bronchoalveolar lavage (BAL) fluid or lung biopsy, as well as those who underwent surgical biopsy, were stained and cultured for bacteria, mycobacteria, and fungi. In addition, polymerase chain reaction (PCR) analysis for BAL specimens and nasal or throat swabs were performed to detect viral organisms. Patients in whom other infectious organisms were identified in the sputum, blood, urine, nasal and throat swabs, BAL fluid, or lung specimen within four weeks of adenovirus identification were regarded to have a concurrent infection and were excluded from this study. Finally, 19 patients confirmed to have only adenovirus pneumonia were included in this study; these patients included the five

patients whose imaging features were published in our previous study (10).

All data including age, sex, premorbid conditions, symptoms, laboratory and pathological findings, clinical course, treatment, and survival outcome were drawn from patient electronic medical records. Patients were regarded as having ARDS when they satisfied the American-European Consensus Conference definition for the condition: acute onset of respiratory failure, bilateral infiltrates on chest radiograph, hypoxemia as defined by a ratio of arterial oxygen partial pressure to fractional inspired oxygen (PaO2/FiO2 ratio) ≤ 200 mm Hg, and no evidence of left atrial hypertension or pulmonary capillary pressure < 18 mm Hg (if measured) to rule out cardiogenic edema (11).

Diagnosis of Adenovirus Pneumonia

Diagnosis was confirmed in five patients based on positive viral culture for adenovirus in BAL fluid. Diagnosis via lung biopsy specimens obtained by video-assisted thoracoscopic surgery (n = 4) or transbronchial lung biopsy (n = 1) was made in another five patients. The specimens were evaluated using hematoxylin and eosin immunohistochemical staining (10, 12). In nine patients, BAL fluid was analyzed using the one-step multiplex real-time AdvanSure RV real-time PCR kit (LG Life Sciences, Seoul, Korea) or conventional multiplex reverse transcription PCR (RT-PCR) assay (Seeplex RV12 Detection Kit; Seegene, Seoul, Korea) (13, 14).

Image Acquisition

Initial chest radiographs and computed tomography (CT) scans were acquired after an average of 4.4 days (range, 0 to 15 days) or 6.1 days (range, 2 to 15 days) from the commencement of symptoms or signs, respectively. The mean time interval between radiologic examination and pathological or microbiological diagnosis was 9.6 days (range, 1–72 days). In one patient whose interval from initial imaging study to pathological diagnosis was 72 days, confirmative diagnosis of adenovirus pneumonia was delayed due to antibiotics treatment showing gradual deterioration of the disease.

Posterior-anterior chest radiographs were obtained with a computed radiography system (FCR 9501; Fuji, Tokyo, Japan) or digital radiography system (Revolution XQi ADS_28.4; GE Medical Systems, Milwaukee, WI, USA) with operating parameters of 70–120 kVp and 2–3 mAs. Serial chest radiographs were acquired for all patients

during hospitalization in order to assess the progression of disease. CT studies were performed using various helical CT scanners (Hi Speed Advantage, Light Speed QXi, Light Speed Ultra, Light Speed VCT and Discovery CT750 HD, GE Healthcare, Chalfont St Giles, England; Brilliance 40, Philips, Best, the Netherlands; Aquilion, Toshiba, Tokyo, Japan). CT scans (114–210 mA, 120 kVp, beam width of 10–20 mm, beam pitch of 1.375–1.5) were performed from the lung apices to the level of the middle portions of both kidneys. Intravenous contrast medium injection was used in approximately half of the patients (10 patients), with 1.5 mL/kg (body weight) of Iomeron 300 (iomeprol, 300 mg iodine/mL; Bracco, Milan, Italy) injected at an infusion rate of 3 mL/s using a power injector (MCT Plus; Medrad, Pittsburgh, PA, USA). The imaging data were reconstructed with section thicknesses of 2.5–5 mm using a bone algorithm. The reconstructed images were then interfaced directly to a picture archiving and communication system (Centricity 3.0; GE Healthcare, Mt. Prospect, IL, USA), which displayed all image data on two monitors (1536 x 2048 matrix, 8-bit viewable gray scale, and 60-ft-lambert luminescence). Both mediastinal (width, 400 HU; level, 20 HU) and lung (width, 1500 HU; level, -700 HU) window images were viewed on these monitors.

Image Analysis

Two chest radiologists (MJC and MJJ, with five and 22 years of experience in chest imaging interpretation, respectively) assessed chest radiographs and CT images; decisions were reached by consensus. The abnormalities on initial chest radiographs were assessed as focal opacity or multifocal or diffuse opacity (15). Parenchymal opacity was defined as an area that appears denser than the surrounding lung tissue without a discrete border. The pattern of the disease course was also identified from sequential chest radiographs as described by Wong et al. (16) and Das et al. (17), where type 1 was radiographic improvement, type 2 was radiographic deterioration by one peak level followed by improvement, type 3 was fluctuating radiographic changes with at least two peaks, and type 4 was progressive radiographic deterioration. Peak level was defined as overall lung parenchymal involvement greater than 25% of the initial extent on radiography.

On CT, the patterns of parenchymal abnormalities were subdivided into areas of ground-glass opacity (GGO), consolidation, and micronodules (< 5 mm in diameter). GGO was defined as an area of hazy increased lung opacity,

within which margins of pulmonary vessels were indistinct. Consolidation was defined as a homogeneous increase in pulmonary parenchymal opacity that obscured the margins of vessels and airway walls (18). The presence of interlobular septal thickening or pleural effusion was also recorded, and the laterality (unilateral vs. bilateral) of the lesions was evaluated. Septal thickening was defined as abnormal widening of an interlobular septum or septa (18). In terms of anatomic location, the distribution of parenchymal abnormalities was classified as central, peripheral, or mixed in the axial plane and upper, lower, or random in the longitudinal plane. The outer third of the lung was defined as peripheral, and the inner two-thirds of the lung were defined as central. The lesions were regarded as distributed in the upper lung zone when they were located above the hilum, in the lower lung zone when they were located below the hilum, or random when the distribution could not be determined. For the acquisition of CT scores, the lung was also divided into upper (above the carina), middle (below the carina and up to the inferior pulmonary vein), and lower (below the inferior pulmonary vein) zones. The involvement of pneumonia within each lung zone was evaluated by scoring each zone from 0 (normal) to 4, with 4 corresponding to nearly total involvement of the lung parenchyma. Total CT scores ranged from 0 to 24 when combined for all six zones (17, 19).

Statistical Analysis

Differences in the clinico-radiological characteristics of the patients who eventually developed ARDS (ARDS group) and those who did not (non-ARDS group) were assessed by using chi-square test, Fisher's exact test, or Student's t test. Statistical analyses were performed with SPSS software (version 19.0; SPSS Inc., Chicago, IL, USA). A p value less than 0.05 was considered to indicate a significant difference.

RESULTS

Demographics and Clinical Characteristics

Detailed patient characteristics are shown in Table 1. Among the 19 patients with adenovirus pneumonia, nine were immunocompromised due to underlying comorbid conditions, such as acute myeloid leukemia (n = 4), non-Hodgkin's lymphoma (n = 1), multiple myeloma (n = 1), lung adenocarcinoma (n = 1), history of liver transplantation for hepatocellular carcinoma (n = 1), and

Table1. Clinical Features and Radiological Findings of 19 Patients with Adenovirus Pneumonia

Patient No.	Age (yr)/Sex	Premorbid Condition	Initial Presentation	Disease Course on X-ray	CT Score	Diagnosis	Progression to ARDS	Time to Progression to ARDS	Antiviral Treatment	Pneumonia-Related Outcome
1	67/M	Lung Cancer	Dyspnea, C/S	Type 2	15	BAL culture	Y	3rd day of illness	No	
2	47/M	AML	Fever, chills, C/S	Type 4	6	TBLB, BAL culture	Y	20th day of illness	Cidofovir	Expired
3	36/F	AML	Dyspnea, cough, BTS	Type 3	3	VATS	N	N/A	Ribavirin	
4	75/F	No	Dyspnea, fever	Type 4	21	VATS	Y	14th day of illness	Ganciclovir	Expired
5	35/F	NHL	Fever, chills, C/S	Type 4	10	VATS	Y	4th day of illness	Ribavirin	Expired
6	67/F	No	Dyspnea	Type 2	12	VATS	Y	11th day of illness	Ribavirin	
7	53/M	AML	Fever, chills	Type 2	11	BAL culture	N	N/A	Cidofovir	
8	55/M	MM	Fever, chills	Type 2	7	BAL culture	N	N/A	No	
9	20/M	No	Dyspnea, fever, sputum	Type 4	12	BAL culture	Y	12th day of illness	Cidofovir	Expired
10	38/F	AML	Fever, dyspnea, C/S	Type 1	3	RT-PCR, BAL culture	N	N/A	Cidofovir	
11	20/M	No	Fever, dyspnea, C/S	Type 1	13	RT-PCR	N	N/A	No	
12	42/M	Liver transplant	Fever, chills	Type 4	20	Real-time PCR	Y	5th day of illness	Cidofovir	Expired
13	23/M	No	Fever, chills, C/S	Type 2	15	Real-time PCR	Y	18th day of illness	Cidofovir	
14	20/M	No	Fever, dyspnea	Type 4	7	Real-time PCR	Y	9th day of illness	Cidofovir	Expired
15	28/M	No	Fever, chills, myalgia	Type 2	13	Real-time PCR	Y	7th day of illness	Cidofovir	
16	19/M	No	Fever, chills, C/S	Type 2	3	Real-time PCR	N	N/A	Cidofovir	
17	20/M	No	Fever, dyspnea	Type 2	11	Real-time PCR	Y	7th day of illness	Cidofovir	
18	51/M	No	Fever, chills, C/S	Type 2	5	Real-time PCR	N	N/A	No	
19	75/M	DM, COPD, ICMP	Dyspnea, C/S	Type 3	12	BAL culture	Y	12th day of illness	Cidofovir	

AML = acute myeloid leukemia, ARDS = acute respiratory distress syndrome, BAL = bronchoalveolar lavage, BTS = blood tinged sputum, COPD = chronic obstructive pulmonary disease, C/S = cough and sputum, DM = diabetes mellitus, ICMP = ischemic cardiomyopathy, MM = multiple myeloma, N/A = not applicable, NHL = non-Hodgkin lymphoma, PCR = polymerase chain reaction, RT-PCR = reverse transcription PCR, TBLB = transbronchial lung biopsy, VATS = video-assisted thoracoscopic surgery

diabetes mellitus in conjunction with chronic obstructive pulmonary disease and ischemic cardiomyopathy (n = 1). In contrast, 10 patients were immunocompetent without underlying disease.

Most patients had upper respiratory symptoms such as dyspnea, cough, sputum, fever, and chills, as shown in Table 1. Twelve of 19 patients (63%) subsequently progressed to ARDS, six (32%) of whom eventually died. The average time of progression from commencement of symptoms or signs to ARDS was 9.6 days, indicating relatively rapid deterioration. Fifteen patients received antiviral therapy, including ganciclovir (n = 1), ribavirin (n = 3), or cidofovir (n = 11).

Radiological Findings

Initial chest radiographs of two patients (11%) were normal, whereas 17 patients had abnormal chest radiographs that showed multifocal or diffuse opacity (n = 8, Fig. 1), or focal opacity (n = 9, Figs. 2, 3). In terms of the disease course identified from serial chest radiographs, two showed gradual improvement (type 1, Fig. 2), nine showed initial radiographic deterioration by one peak level followed by improvement (type 2), two showed radiographic fluctuations with at least two peaks (type 3), and six patients showed progressive radiographic deterioration (type 4, Figs. 1, 3).

Patterns and distribution of CT findings are summarized in Table 2. The most frequent CT appearance was GGO, which was seen in all patients (n = 19), combined with other patterns such as consolidation (n = 14) and micronodules (n = 3). Parenchymal abnormalities were distributed bilaterally in 17 patients (Figs. 1, 2), whereas unilateral involvement was seen in two patients (Fig. 3). Interlobular septal thickening was demonstrated in 12 patients, and pleural effusion was present in 11 patients. The average number of lobes involved was 4.2 ± 1.4 (range, 1 to 5). Pulmonary abnormalities showed upper lung zone predominance in four patients (21%) and lower lung zone predominance in six patients (32%). However, nine patients (47%) showed random parenchymal involvement without zonal predominance. In terms of axial distribution, most of the cases (79%) showed mixed central and peripheral involvement.

## Comparisons between ARDS and Non-ARDS Groups

Table 3 shows the comparison between the ARDS and non-ARDS groups according to clinical and radiological findings. No significant differences between the groups were identified for the clinical variables of patient age (p = 0.651), sex (p = 0.998), or presence of premorbid
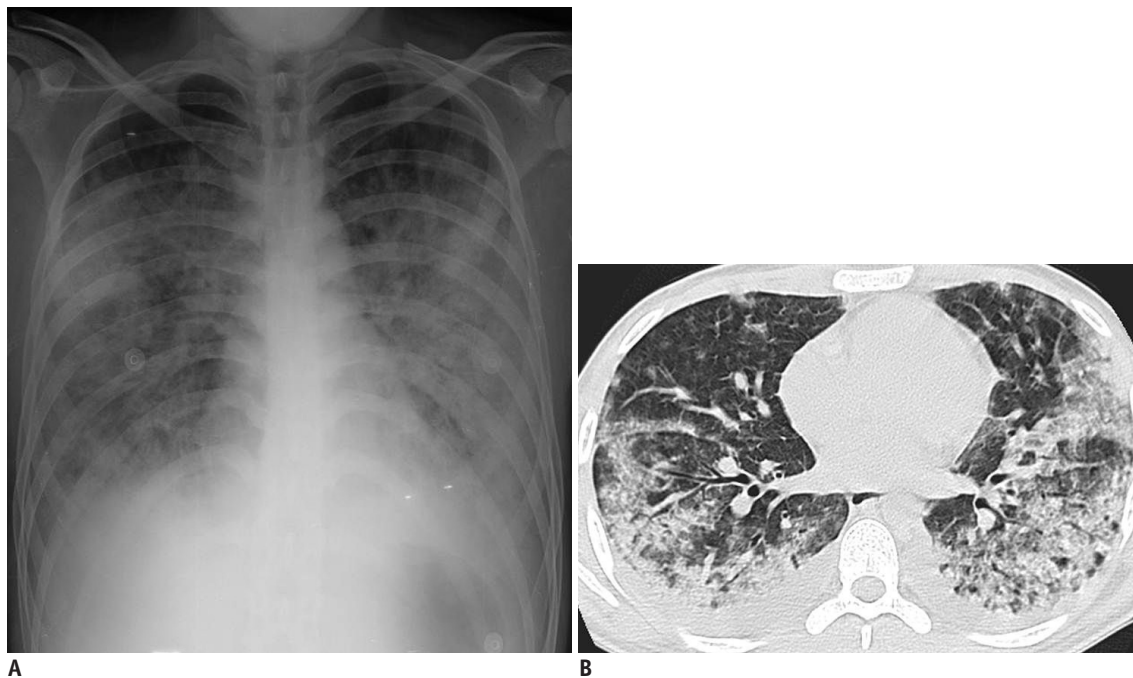
Fig. 1. 20-year-old immunocompetent man complaining of fever, dyspnea, productive cough, and sputum.
He visited our hospital on 10th day from onset of his symptoms, which were abruptly aggravated two days prior. **A.** Chest radiograph demonstrates multifocal or diffuse opacity. **B.** Chest CT scan obtained on same day demonstrates extensive airspace lesions in both lungs, with bilateral pleural effusions. Total CT score was 13. Culture of BAL fluid helped confirm adenovirus pneumonia. On next day, patient was transferred to intensive care unit, and he eventually expired on 21st day of hospitalization. BAL = bronchoalveolar lavage, CT = computed tomography
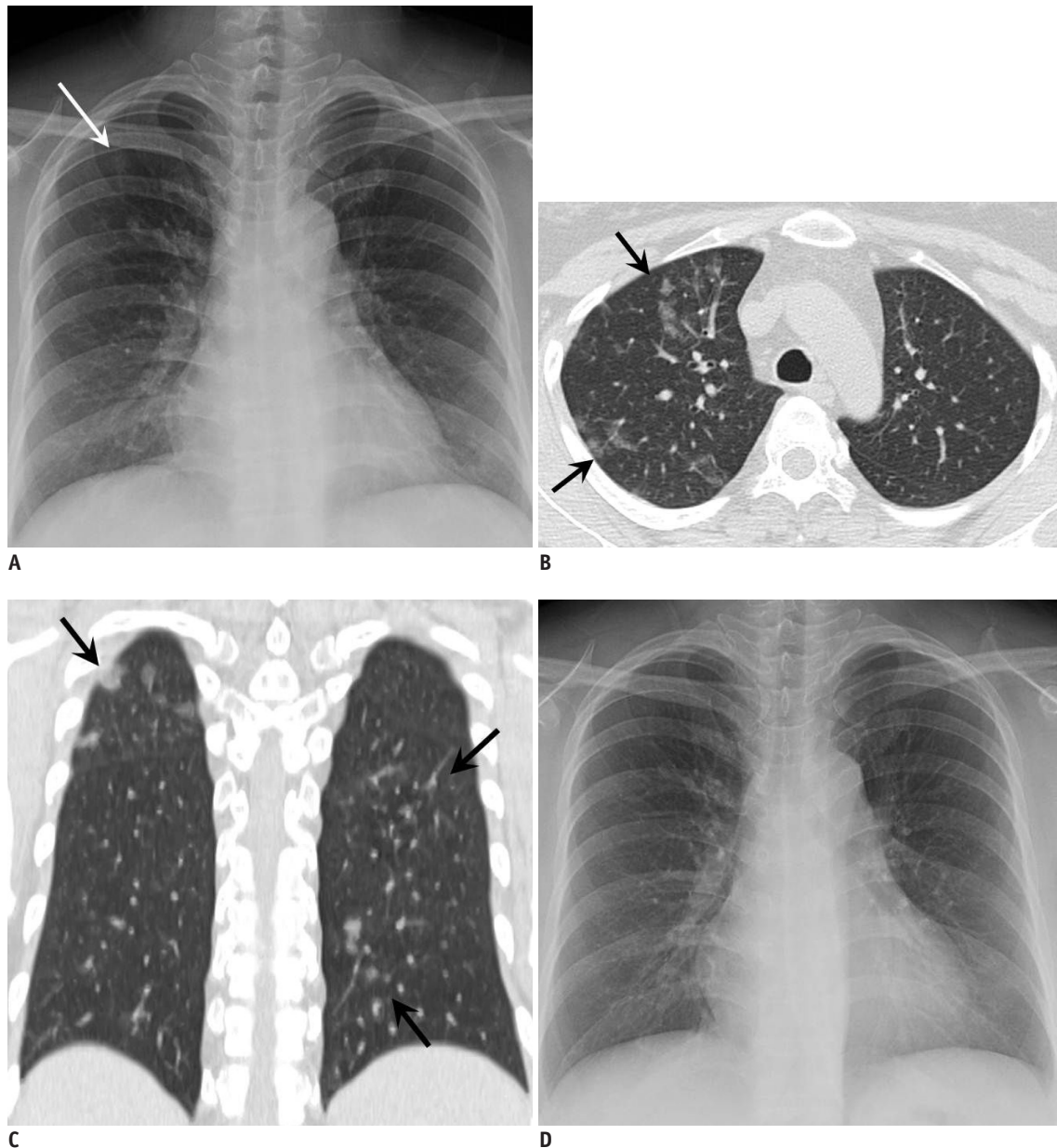
Fig. 2. 38-year-old woman with acute myelogenous leukemia visited our institution for aggravated fever, cough, sputum, and dyspnea for four days.
A. Chest radiograph at admission demonstrates subtle focal opacity in right upper lung zone (white arrow). **B, C.** Chest CT scans obtained on same day demonstrate patchy peribronchial ground-glass opacity in both lungs (black arrows). Total CT score was 3. Culture and RT-PCR of BAL fluid confirmed adenovirus pneumonia. **D.** Follow-up chest radiograph obtained after two weeks of treatment with cidofovir demonstrates disappearance of focal opacity in right upper lung zone, suggesting type 1 disease pattern. BAL = bronchoalveolar lavage, CT = computed tomography, RT-PCR = reverse transcription polymerase chain reaction

conditions (p = 0.650). Regarding the radiological findings, there was no significant difference in initial radiograph findings (p = 0.813), but the radiographic pattern of disease course differed significantly between the ARDS and non-ARDS groups (p = 0.048). In the non-ARDS group, types 1 and 2 accounted for more than 85% of patients, and no one was classified as type 4. In contrast, half of the patients in the ARDS group showed progressive deterioration of

chest radiographs and were classified as type 4. Among the CT findings, the presence of pleural effusion and total CT scores differed significantly (p = 0.010 and p = 0.007, respectively) between the two groups. Patients who progressed to ARDS showed higher total CT scores and a higher probability of pleural effusion. Other CT features, such as laterality (p = 0.998), presence of consolidation (p = 0.305) and micronodules (p = 0.997), inter- or
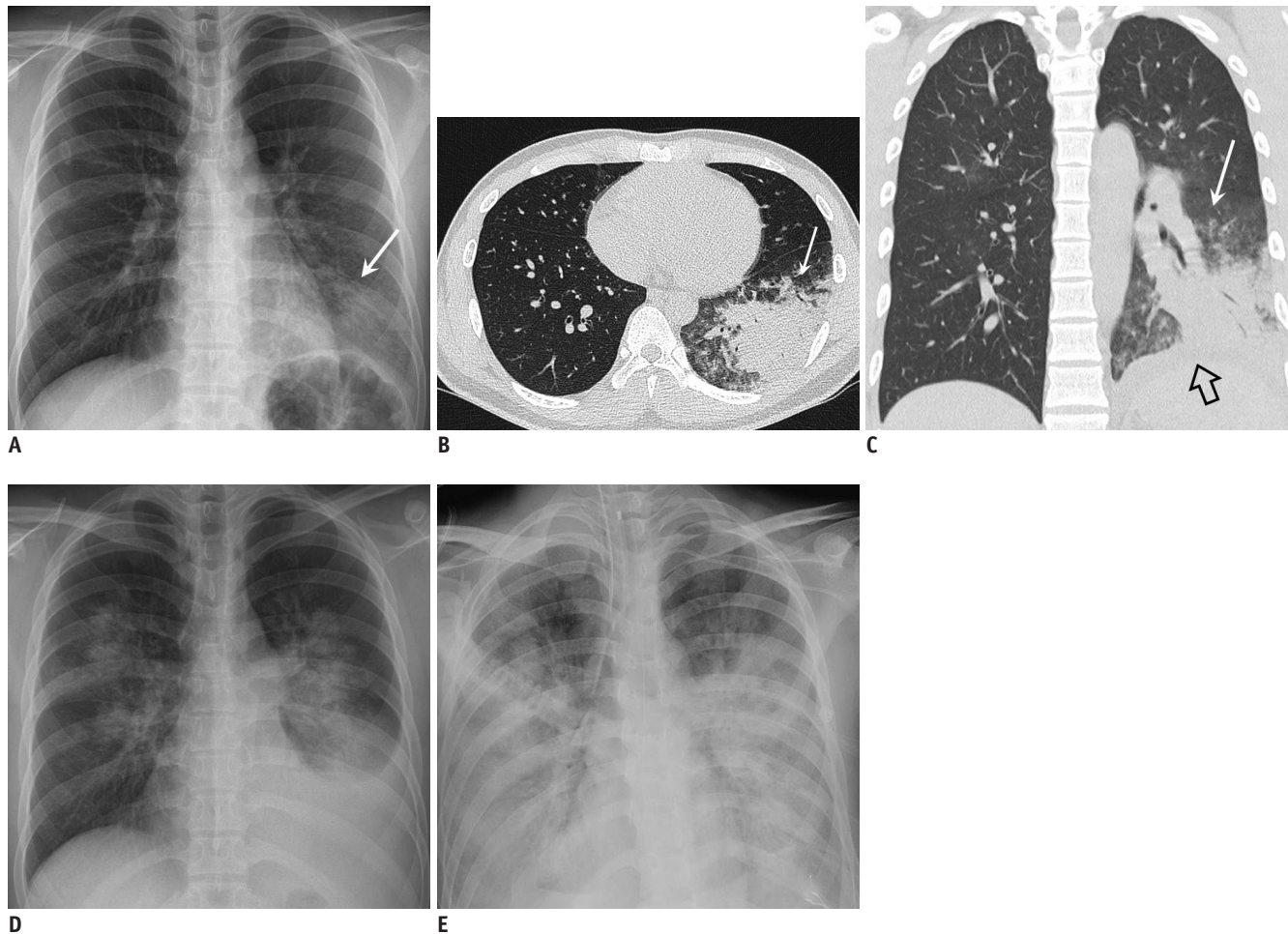
Fig. 3. 20-year-old immunocompetent man suffering from acute fever and dyspnea.
A. Chest radiograph obtained on fifth day of illness demonstrates focal opacity in left lower lobe (arrow). **B, C.** Chest CT scans demonstrate dense consolidation and ground-glass opacity in left lower lobe (arrow). Small left pleural effusion is indicated by open arrow. Total CT score was 7. **D.** Chest radiograph obtained on seventh day of illness demonstrates increased amount of left pleural effusion and bilateral multifocal areas of parenchymal opacity. **E.** Progressive diffuse opacity in both lungs and bilateral pleural effusions are shown on follow-up radiograph taken on 13th day, suggesting ARDS and type 4 disease pattern. Patient expired on 16th day of illness. ARDS = acute respiratory distress syndrome, CT = computed tomography

intralobular septal thickening (p = 0.656), and number of involved lobes (p = 0.973) did not differ significantly between the ARDS and non-ARDS groups.

DISCUSSION

In our study, progression to respiratory failure was unpredictable, showing relatively high rates (12 of 19 patients, 63%) and rapid deterioration. There were no significant differences in baseline clinical characteristics between the ARDS and non-ARDS groups. This result is different from previous reports indicating that geriatric immunocompromised patients are more prone to pneumonia and to developing ARDS than are young immunocompetent patients (20-22). Our study suggests that, if adenovirus

infection manifests as airspace lesions on chest radiograph or CT, aggressive treatment and careful follow-up should be carried out, regardless of patient age and premorbid conditions; patients with these conditions showed a rapid progression of the disease to ARDS.

Our study also demonstrated that the disease extent seen on chest CT, which was defined by total CT score and the presence of pleural effusion significantly differed between the ARDS and non-ARDS groups (Fig. 1). In addition, the patients in the ARDS group showed progressive deterioration on sequential radiographs, rather than fluctuations or improvement. This result is consistent with previous reports regarding prognoses of other viral pneumonias such as H1N1, severe acute respiratory syndrome, and Middle East respiratory syndrome (16, 17, 23). Close imaging follow-

Table 2. Patterns and Distribution of CT Findings in 19 Patients with Adenovirus Pneumonia

CT Pattern	Laterality		Longitudinal Zone			Axial Distribution		
	Unilateral	Bilateral	Upper	Lower	Random	Central	Peripheral	Mixed
Ground-glass opacity (n = 19 [100%])	2	17	4	6	9	1	3	15
Consolidation (n = 14 [74%])	2	12	2	6	6	0	3	11
Micronodules (n = 3 [15%])	0	3	1	0	2	1	0	2
Inter/intralobular septal thickening (n = 12 [63%])	1	11	2	4	6	1	0	11

CT = computed tomography

Table 3. Comparison of ARDS and Non-ARDS Groups according to Clinical and Radiological Factors

Characteristics	All (n = 19)	ARDS Group (n = 12)	Non-ARDS Group (n = 7)	P
Age (yr)	41.6 ± 19.1	43.3 ± 22.3	38.9 ± 15.1	0.651
Premorbid conditions (%)	8 (42)	5 (42)	4 (57)	0.650
Initial radiographic findings (%)				0.813
Normal	2 (11)	1 (8)	1 (14)	
Focal opacity	9 (47)	5 (42)	4 (57)	
Multifocal/diffuse opacity	8 (42)	6 (50)	2 (29)	
Radiographic disease course (%)				0.048
Type 1	2 (11)	0 (0)	2 (29)	
Type 2	9 (47)	5 (42)	4 (57)	
Type 3	2 (11)	1 (8)	1 (14)	
Type 4	6 (31)	6 (50)	0 (0)	
CT findings				
Unilateral/bilateral (%)	2 (11)/17 (89)	1 (8)/11 (92)	1 (14)/6 (86)	0.998
Ground-glass opacity (%)	19 (100)	12 (100)	7 (100)	N/A
Consolidation (%)	14 (74)	10 (83)	4 (57)	0.305
Micronodules (%)	3 (16)	2 (17)	1 (14)	0.997
Inter/intralobular septal thickening (%)	12 (63)	7 (58)	5 (71)	0.656
Pleural effusion (%)	13 (68)	11 (92)	2 (29)	0.010
Number of the involved lobes	4.2 ± 1.4	4.2 ± 1.6	4.1 ± 1.2	0.973
Total CT score	9.2 ± 4.8	12.8 ± 4.5	6.4 ± 4.1	0.007

ARDS = acute respiratory distress syndrome, CT = computed tomography, N/A = not applicable

up for the evaluation of disease progression should be a requisite in managing patients with adenovirus pneumonia.

One can argue that the rate of respiratory failure in adenovirus pneumonia might have been overestimated in our study, considering the way that adenovirus pneumonia was confirmed. The effort for confirmatory diagnosis was usually made when the results of laboratory evaluations, including the staining and culture of blood, urine, and sputum, were negative, and the response to empirical antibiotic therapy was unsatisfactory. Thus, the diagnosis might have been delayed, missing the important opportunity for timely treatment. In addition, our institution is a tertiary referral hospital in Seoul; thus, the rates of ARDS and mortality could be further exaggerated. We admit that the rates of ARDS and mortality of adenovirus

pneumonia in our study might not be applicable to those of adenovirus pneumonia in the general community. Nevertheless, we think that our results are meaningful with respect to emphasizing the severity of adenovirus pneumonia.

It is curious that adenovirus pneumonia developed into ARDS with such a high percentage in our study. It is known that adenovirus causes cytolysis, which accounts for tissue damage, and damaged pulmonary capillaries can contribute to respiratory failure (24). Another possible explanation is the unregulated complement activation, producing C5a and resulting in activation of phagocytic cells, generation of oxidants, release of histones, and, eventually, a cytokine storm (25, 26). Many previous cases of respiratory failure resulting from influenza A viruses H1N1, H5N1, and H7N9,

severe acute respiratory syndrome coronavirus, and Middle East respiratory syndrome coronavirus pneumonia were associated with cytokine storms (27). Similar to these highly pathogenic viruses which have been severe threats to public health, adenovirus might have triggered cytokine storms in patients who progressed to ARDS. However, it is still difficult to explain why some individuals are susceptible to systemic inflammation, whereas others are resistant to it. Further studies should be performed to identify the viral determinants and genetic factors associated with ARDS, and to better understand the pathophysiology of adenovirus infection.

In terms of the radiological findings of adenovirus pneumonia, the CT features were so diverse that it was difficult to define specific findings for adenovirus pneumonia. Although the most common CT feature was bilateral ground-glass opacities, the findings were variable, from unilateral lobar consolidation to clustered micronodules. With regard to the initial chest radiographic findings, two patients (11%) were normal, while focal opacity was noted in nine patients (47%). Despite the well-known imaging features of viral pneumonia, which causes diffuse and bilateral interstitial involvement (28), two patients in our study presented with unilateral consolidation and GGO with or without pleural effusion. Features of focal opacity on chest radiograph and unilateral dense consolidation on CT were likely to be interpreted as community-acquired pneumonia. In fact, there have been several reports describing adenovirus pneumonias that have presented with unilateral lobar infiltrates (6, 8, 20). Thus, we should not discard the possibility of adenoviral pneumonia in patients suspected of having an acute lower respiratory tract infection with unilateral airspace lesion, especially when response to antibiotics was ineffective, and sputum Gram stain and culture were negative for bacterial infection. Every effort should be made to achieve a confirmative diagnosis and timely treatment in such cases.

There are limitations to our study. First, our study was retrospective in nature and thus had a selection bias. Patients with adenovirus pneumonia who had severe respiratory symptoms or abnormal radiologic findings might have been selectively included. Second, we did not perform a serotype analysis of adenovirus. To date, more than 52 serotypes of adenovirus have been recognized and are known to show different biological properties (29). Further work needs to be performed investigating the virulent strains of adenovirus, particularly with regard to radiologic

appearance, disease extent, and severity. Third, the time to CT acquisition from symptom onset was heterogeneous, ranging from two to 15 days. CT scans from the ARDS group might have progressed from an initially mild disease to showing a relatively large extent of involvement. Fourth, we simplified the chest radiographic abnormality as focal, multifocal, and diffuse opacity without assessing other findings such as interstitial opacities. However, we were more focused on the disease extent and sequential radiographic changes rather than detailed radiographic findings. Fifth, our study only included patients confirmed to have adenovirus pneumonia and did not include a comparison group. Sixth, the diagnosis of adenovirus pneumonia was made using various methods. Lastly, the number of cases in the present study is small, and a large-scale prospective study is needed. In addition, comparison of clinico-radiological features between immunocompromised and immunocompetent patients with adenovirus pneumonia would also have clinical implications toward understanding the clinical course of the disease.

In conclusion, our study demonstrates that adenovirus pneumonia is associated with high rates of ARDS and mortality in the single tertiary care setting. Adenovirus pneumonia usually manifests as multifocal or diffuse opacity on chest radiographs, and bilateral GGO and consolidation with or without pleural effusion on CT. However, we should remember that adenovirus pneumonia can also present as focal opacity with unilateral airspace lesions. Patients with adenovirus pneumonia demonstrate subsequent rapid deterioration to ARDS regardless of age and premorbid conditions; thus, aggressive treatment and careful follow-up are mandatory. In particular, patients who have progressed to ARDS are prone to show a large disease extent and high probability of pleural effusion on CT, supporting the importance of intensive imaging follow-up in patients suffering from adenovirus pneumonia.

REFERENCES

1. Han BK, Son JA, Yoon HK, Lee SI. Epidemic adenoviral lower respiratory tract infection in pediatric patients: radiographic and clinical characteristics. *AJR Am J Roentgenol* 1998;170:1077-1080
2. Krilov LR, Rubin LG, Frogel M, Gloster E, Ni K, Kaplan M, et al. Disseminated adenovirus infection with hepatic necrosis in patients with human immunodeficiency virus infection and other immunodeficiency states. *Rev Infect Dis* 1990;12:303-307

3. Echavarria MS, Ray SC, Ambinder R, Dumler JS, Charache P. PCR detection of adenovirus in a bone marrow transplant recipient: hemorrhagic cystitis as a presenting manifestation of disseminated disease. *J Clin Microbiol* 1999;37:686-689

4. Landry ML, Fong CK, Neddermann K, Solomon L, Hsiung GD. Disseminated adenovirus infection in an immunocompromised host. Pitfalls in diagnosis. *Am J Med* 1987;83:555-559

5. Ardehali H, Volmar K, Roberts C, Forman M, Becker LC. Fatal disseminated adenoviral infection in a renal transplant patient. *Transplantation* 2001;71:998-999

6. Klinger JR, Sanchez MP, Curtin LA, Durkin M, Matyas B. Multiple cases of life-threatening adenovirus pneumonia in a mental health care center. *Am J Respir Crit Care Med* 1998;157:645-649

7. Tate JE, Bunning ML, Lott L, Lu X, Su J, Metzgar D, et al. Outbreak of severe respiratory disease associated with emergent human adenovirus serotype 14 at a US air force training facility in 2007. *J Infect Dis* 2009;199:1419-1426

8. Bryant RE, Rhoades ER. Clinical features of adenoviral pneumonia in Air Force recruits. *Am Rev Respir Dis* 1967;96:717-723

9. Hwang SM, Park DE, Yang YI, Park SJ, Lee HK, Kim MJ, et al. Outbreak of febrile respiratory illness caused by adenovirus at a South Korean military training facility: clinical and radiological characteristics of adenovirus pneumonia. *Jpn J Infect Dis* 2013;66:359-365

10. Chong S, Lee KS, Kim TS, Chung MJ, Chung MP, Han J. Adenovirus pneumonia in adults: radiographic and high-resolution CT findings in five patients. *AJR Am J Roentgenol* 2006;186:1288-1293

11. Bernard GR, Artigas A, Brigham KL, Carlet J, Falke K, Hudson L, et al. The American-European Consensus Conference on ARDS. Definitions, mechanisms, relevant outcomes, and clinical trial coordination. *Am J Respir Crit Care Med* 1994;149(3 Pt 1):818-824

12. Montgomery EA, Popek EJ. Intussusception, adenovirus, and children: a brief reaffirmation. *Hum Pathol* 1994;25:169-174

13. Rheem I, Park J, Kim TH, Kim JW. Evaluation of a multiplex real-time PCR assay for the detection of respiratory viruses in clinical specimens. *Ann Lab Med* 2012;32:399-406

14. Mahony J, Chong S, Merante F, Yaghoubian S, Sinha T, Lisle C, et al. Development of a respiratory virus panel test for detection of twenty human respiratory viruses by use of multiplex PCR and a fluid microbead-based assay. *J Clin Microbiol* 2007;45:2965-2970

15. Paul NS, Roberts H, Butany J, Chung T, Gold W, Mehta S, et al. Radiologic pattern of disease in patients with severe acute respiratory syndrome: the Toronto experience. *Radiographics* 2004;24:553-563

16. Wong KT, Antonio GE, Hui DS, Lee N, Yuen EH, Wu A, et al. Thin-section CT of severe acute respiratory syndrome: evaluation of 73 patients exposed to or with the disease. *Radiology* 2003;228:395-400

17. Das KM, Lee EY, Enani MA, AlJawder SE, Singh R, Bashir S, et al. CT correlation with outcomes in 15 patients with acute Middle East respiratory syndrome coronavirus. *AJR Am J Roentgenol* 2015;204:736-742

18. Hansell DM, Bankier AA, MacMahon H, McLoud TC, Müller NL, Remy J. Fleischner Society: glossary of terms for thoracic imaging. *Radiology* 2008;246:697-722

19. Ooi GC, Khong PL, Müller NL, Yiu WC, Zhou LJ, Ho JC, et al. Severe acute respiratory syndrome: temporal lung changes at thin-section CT in 30 patients. *Radiology* 2004;230:836-844

20. Dudding BA, Wagner SC, Zeller JA, Gmelich JT, French GR, Top FH Jr. Fatal pneumonia associated with adenovirus type 7 in three military trainees. *N Engl J Med* 1972;286:1289-1292

21. Zahradnik JM, Spencer MJ, Porter DD. Adenovirus infection in the immunocompromised patient. *Am J Med* 1980;68:725-732

22. Retalis P, Strange C, Harley R. The spectrum of adult adenovirus pneumonia. *Chest* 1996;109:1656-1657

23. Kang H, Lee KS, Jeong YJ, Lee HY, Kim KI, Nam KJ. Computed tomography findings of influenza A (H1N1) pneumonia in adults: pattern analysis and prognostic comparisons. *J Comput Assist Tomogr* 2012;36:285-290

24. Hakim FA, Tleyjeh IM. Severe adenovirus pneumonia in immunocompetent adults: a case report and review of the literature. *Eur J Clin Microbiol Infect Dis* 2008;27:153-158

25. Guo RF, Ward PA. Role of C5a in inflammatory responses. *Annu Rev Immunol* 2005;23:821-852

26. Wang R, Xiao H, Guo R, Li Y, Shen B. The role of C5a in acute lung injury induced by highly pathogenic viral infections. *Emerg Microbes Infect* 2015;4:e28

27. Tisoncik JR, Korth MJ, Simmons CP, Farrar J, Martin TR, Katze MG. Into the eye of the cytokine storm. *Microbiol Mol Biol Rev* 2012;76:16-32

28. Franquet T. Imaging of pulmonary viral pneumonia. *Radiology* 2011;260:18-39

29. Louie JK, Kajon AE, Holodniy M, Guardia-LaBar L, Lee B, Petru AM, et al. Severe pneumonia due to adenovirus serotype 14: a new respiratory threat?. *Clin Infect Dis* 2008;46:421-425